The East Asian Jet Stream and Asian-Pacific-American Climate

Song Yang*, K.-M. Lau, and K.-M. Kim**

NASA/Goddard Space Flight Center
Laboratory for Atmospheres
Climate and Radiation Branch
Greenbelt, Maryland 20771, USA

1. Introduction

The upper-tropospheric westerly jet stream over subtropical East Asia and western Pacific, often referred to as East Asian Jet (EAJ), is an important atmospheric circulation system in the Asian-Pacific-American (APA) region during winter. It is characterized by variabilities on a wide range of time scales and exerts a strong impact on the weather and climate of the region. On the synoptic scale, the jet stream is closely linked to many phenomena such as cyclogenesis, frontogenesis, blocking, storm track activity, and the development of other atmospheric disturbances. On the seasonal time scale, the variation of the EAJ determines many characteristics of the seasonal transition of the atmospheric circulation especially over East Asia. The variabilities of the EAJ on these time scales have been relatively well documented (e.g., Yeh et al. 1959, Palmén and Newton 1969; Zeng 1979).

It has also been understood since decades ago that the interannual variability of the EAJ is associated with many climate signals in the APA region. These signals include the persistent anomalies of the East Asian winter monsoon and the changes in diabatic heating and in the Hadley circulation (Bjerknes 1966; Chang and Lau 1980; Huang and Gambo 1982; Kang and Held 1986; Tao and Chen 1987; Lau et al. 1988; Yang and Webster 1990; Ding 1992; Webster and Yang 1992; Dong et al. 1999). However, many questions remain for the year-to-year variabilities of the EAJ and their relation to the APA climate. For example, what is the relationship between the EAJ and El Nino/Southern Oscillation (ENSO)? Will the EAJ and ENSO play different roles in modulating the APA climate? How is the jet stream linked to the non-ENSO-related sea surface temperature (SST) anomalies and to the Pacific/North American (PNA) teleconnection pattern?

In this study, we address several issues related to the wintertime EAJ with a focus on interannual time scales. We will examine the association between the jet stream and ENSO, which has always been overshadowed by the relationship between ENSO and the upper-tropospheric winds over northern extratropics of the central Pacific. The relative contributions of the EAJ and ENSO to Asian-Pacific climate anomalies will be discussed. We will investigate the linkage of the EAJ to variabilities of the Asian winter monsoon, tropical convection, and upper tropospheric wave patterns. We will also explore the relationship between the EAJ and extratropical SST with an aim at providing useful information for improving our understanding of the connection of the EAJ to surface boundary conditions.

2. Data

The primary data set used in this study is the reanalysis product from the US NOAA National Centers for Environmental Prediction and National Center for Atmospheric Research. Other data include the surface air temperature from US NASA Goddard Institute for Space Studies, precipitation from Global Precipitation Climatology Project, and the snow cover data from NOAA. The NOAA reconstructed SST and Southern Oscillation index (SOI) are also analyzed. These data sets cover different time periods and are distributed in different spatial resolutions. In this study, seasonal averages, computed from monthly mean data, are analyzed with an emphasis on the December-January-February (DJF) averaged values.

3. Results

3.1 ENSO and EAJ related circulation patterns

During the northern winter, the largest values of global 200 mb zonal wind (U200) exist over East Asia, with a center larger than 70 ms^{-1} over the ocean south of Japan. However, the maximum variances of U200 do not occur within the maximum centers of the wind but emerge from the tropics and

subtropics of the central–eastern Pacific and the North Atlantic east of Canada. The variability of U200 is actually small over entire Asia. Figure 1a shows that the variations of the U200 maxima over East Asia are not strongly related to ENSO. The correlation between SOI and the wind near the EAJ core is close to zero. The winds over subtropical Asia and Pacific west of the dateline have little link to the Southern Oscillation.
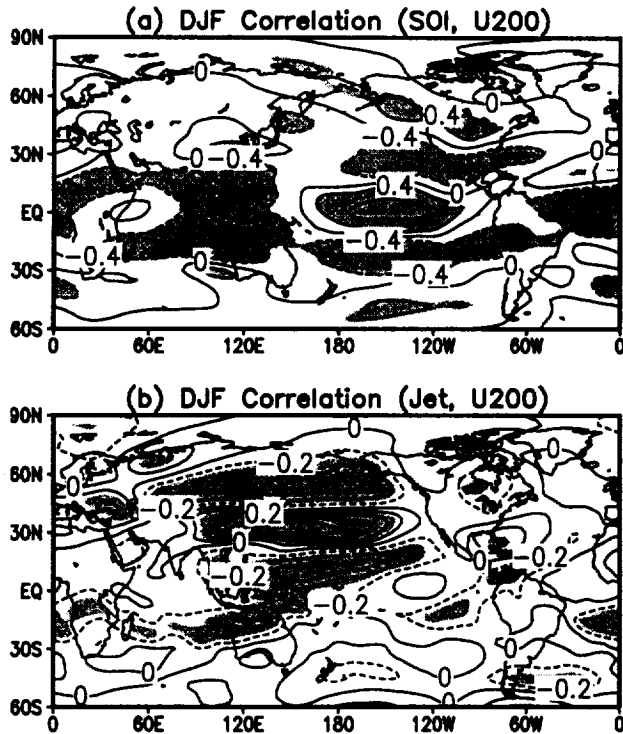

(a) DJF Correlation (SOI, U200)

(b) DJF Correlation (Jet, U200)

Fig. 1. (a) DJF correlation between SOI and NCEP/NCAR reanlaysis U200 for 1949–99. (b) DJF correlation between the EAJ and U200. Contour intervals: 0.4 in (a) and 0.2 in (b).

Out of the 50 DJFs from 1949 to 1999, the EAJ maximum appears over 32.5°N, 140°E in 15 DJFs. Its maximum is mostly located over 32.5°N and shifts occasionally northward to 35°N. Longitudinally, this maximum shifts westward or eastward by about 10 degrees. The small migration of the EAJ, especially latitudinally, facilitates the construction of an index that measures the variability of the jet stream. We define this index as the yearly DJF U200 averaged within 30–35°N and 125–165°E. The correlation between this EAJ index and the global grid–point U200 is presented in Fig. 1b. The dominant feature of the figure is that the intensification of the EAJ is accompanied by a reduction of westerly component over the northern

extratropics from southeastern Russia to the Bering Sea and over the tropical Pacific Ocean. (The tropical easterlies also intensify, though not significantly, when the EAJ becomes stronger.) The strengthening EAJ core increases the U200 upstream and downstream, although the downstream intensification is more obvious. Importantly, the pattern of Fig. 1b is substantially different from the ENSO–related pattern shown in Fig. 1a. Besides the signal over the tropical monsoon region of Asia–Australia, the ENSO–related features over the Pacific are mainly limited to the east of the dateline. On the contrary, the signals that are related to the EAJ appear mainly over East Asia and the western–central Pacific. At the locations where EAJ–U200 correlation is strongest, the SOI–U200 correlation is among the weakest. Thus, the teleconnection pattern linked to the EAJ is clearly distinct from that associated with ENSO, indicating that the EAJ and ENSO link to two different modes of the atmospheric circulation in the APA region.

The features discussed above are confirmed by the empirical orthogonal function (EOF) analysis for U200 (figures not shown). The first EOF mode captures the ENSO–related feature that involves an increase in the subtropical central Pacific U200 during El Niño winters and a decrease in the wind during La Niña winters. The second mode exhibits northwest–southeast oriented signals extending from extratropical Asia to the tropical central Pacific Ocean, similar to those shown in Fig. 1b.

Since the two EOF modes measure respectively the ENSO and EAJ related patterns, we can assess the relative importance of ENSO and EAJ for the APA climate by analyzing the relations of the two modes to the climate. Figure 2 shows the pattern of regressions of 850 mb wind vectors against the first and second principal components from the above EOF analysis. (The shadings indicate the areas over which the correlation between the principal component and the wind component, either zonal, meridional, or both, is significant at the 99% confidence level.) There exist several differences between the two panels of Fig. 2. In spite of the similarity over the extratropical Pacific north of 25°N and east of 150°E, the changes associated with the increase in the westerlies over subtropical central Pacific (Fig. 2a) are nearly in an opposite sign with those linked to the EAJ intensification (Fig. 2b). Figure 2a shows a decrease in the trade winds over the tropical central Pacific and in the westerlies over the tropical Indian ocean,

which causes a "divergence" over Indonesia and the tropical western Pacific. However, the trade winds and the westerlies become stronger when the EAJ is strong. An area of "convergence" appears over Southeast Asia including the South China Sea, consistent with the increase in local convection and precipitation (figures not shown). During El Niño years, the Asian winter monsoon becomes slightly weaker, together with a clockwise pattern over southern Asia and the nearby oceans (Fig. 2a). However, when the EAJ is strong, the East Asian winter monsoon intensifies significantly. In particular, the northerly component over East Asia and the western Pacific strengthens from the mid-latitudes to the tropics (Fig. 2b). The figure also shows that the change in the monsoon is part of the broad-scale counterclockwise pattern over the North Pacific. A remarkable feature of Fig. 2 is that while the first principal component links clearly to dominant signals over the central-eastern Pacific, the second principal component is strongly associated with the signals over the western Pacific.
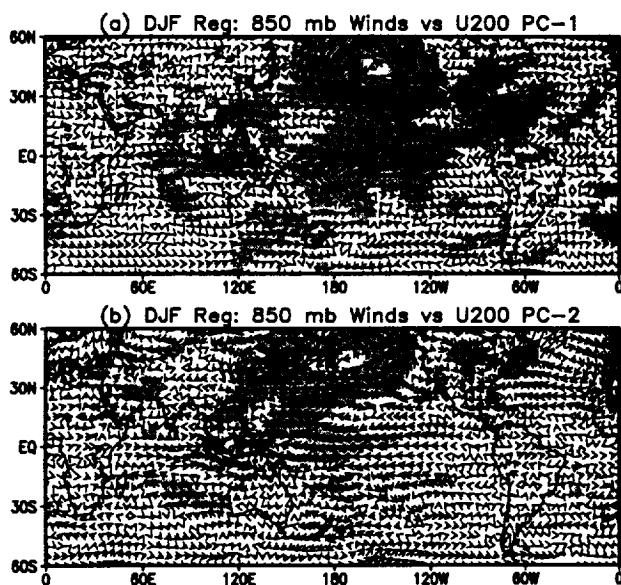

Fig.2. (a) DJF regressions (in m/s) of 850 mb winds against the first principal component from the U200 EOF analysis. (b) Same as (a), but for the second principal component.

3.2 EAJ's climate impact

It has been presented in Fig. 2 that, compared with ENSO, the EAJ is more strongly linked to the East Asian winter monsoon. For the period from 1950-99, the correlation between the EAJ and the 850 mb meridional wind averaged over 20-40°N,

100-140°E is -0.51. However, the correlation between SOI and the area-averaged wind is only -0.37.

Here, we will expose the influence of the EAJ on the APA climate by demonstrating more features in composite patterns. Figure 3 shows the changes, between the strong and weak EAJs, in 500 mb geopotential height (H500), stationary wave activity flux (SWAF), and snow cover. The year-to-year variability of the intensity of the EAJ is associated with significant change in the atmospheric wave pattern in the APA region. Two important features associated with strong EAJ can be found in Fig. 3a. Firstly, the East Asian Trough deepens and H500 decreases to its east but increases to its west. Thus, the change in the EAJ is accompanied by an adjustment of the large-scale circulation system over Asia and the Pacific. This adjustment increases the north-south pressure gradient in the Asian-Pacific region and favors a southeastward intrusion of the cold air from Siberia, intensifying the East Asian winter monsoon. Secondly, associated with the strong jet stream is a stronger PNA pattern, which links closely to the climate of eastern Pacific and North America.

Figure 3b shows the change in SWAF (Plumb 1985) between the strong and weak EAJs. Following Yang and Gutowski (1994), we reveal the features of the horizontal components at 300 mb (vectors) and the vertical component at 850 mb (contours and shadings). In both strong and weak EAJ cases, the wave activities propagate mainly eastward and upward. They emanate from eastern Asia, the eastern Pacific, and western Atlantic. Obviously, the wave activities propagate southward from these three locations. When the EAJ weakens, the wave activities diminish in almost entire northern extratropics. Major reduction occurs in the eastward propagation over East Asia, the southeastward propagation over the eastern Pacific and the Atlantic, and the northeastward propagation over North America. Also reduced remarkably is the upward propagation over East Asia and the eastern Pacific. When the EAJ is weak, the northeastward propagation of the SWAF over East Asia north of 40°N weakens as well. This weakening is consistently accompanied by an intensification of the upward propagation over the Sea of Okhotsk and nearby regions. Figure 3b suggests a teleconnection between EAJ and the atmospheric circulation over the eastern Pacific, North America, and even the Atlantic Ocean.
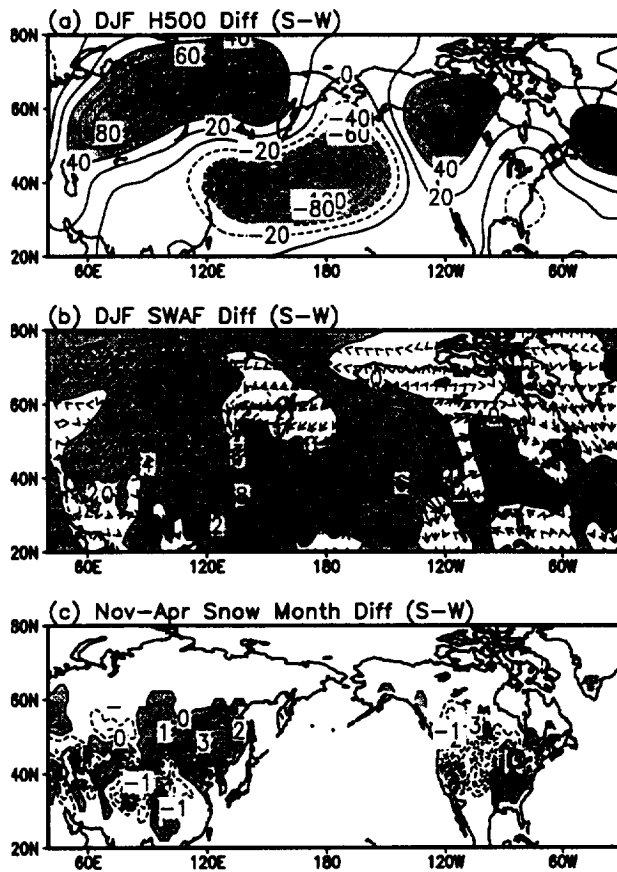
(a) DJF H500 Diff (S-W)

(b) DJF SWAF Diff (S-W)

(c) Nov-Apr Snow Month Diff (S-W)

(a) U200   MODE 2 (14.0%)

(b) SST

(c) PC

R = 0.79

——— U200   ------- SST

Fig.3. Differences, between strong and weak EAJs, in the number of month of H500 (a; in m), SWAF (b), and snow cover (c; in month). In (b), the vectors are for 300 mb horizontal component and the contours and shadings for 850 mb vertical component (see text for units).
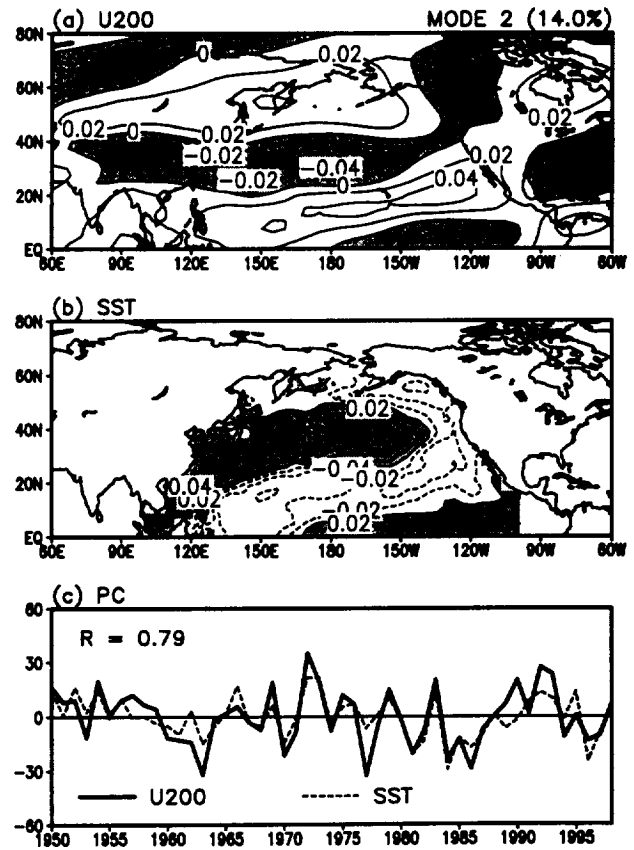
Fig. 4. The second mode of SVD of the northern hemisphere U200 (a) and North Pacific SST (b) for DJF, together with the corresponding time series (c).

Figure 3c provides information about the EAJ—related changes in snow area and frequency. The value shown for each grid is the difference, between the strong and weak EAJs, in the number of months when snow is present. Data from the November–April of six years of strong EAJ and six years of weak EAJ are used in the calculation. For example, the number "5" at a specific grid means that snow exists in that grid more frequently in the strong EAJ group than in the weak EAJ group by five months. The figure indicates that, when the EAJ is strong, snow appears more frequently and extensively over Asia, mainly between 37°N and 55°N. Figure 3c also indicates that strong EAJs link to less (more) frequent snow over the western (eastern) United States, suggesting a link between an East Asian system and North American climate.

3.3 Linkage of EAJ to North Pacific SST

We now explore the relationship between the EAJ and the Earth's surface conditions. Since there is no apparent connection between the EAJ and ENSO, or Niño–3 SST, we examine the relationship of the jet stream with the SST of other ocean domains. Figure 3a has shown a strong relationship between the EAJ and PNA pattern, which has been previously known to link with the extratropical North Pacific SST (NPSST; e.g., Kawamura 1994; Deser and Blackmon 1995). Thus, we apply the singular value decomposition (SVD) analysis to study the association between the EAJ and NPSST. Figure 4, where the second SVD mode is shown, indicates a close relationship between the EAJ and the SST of extratropical Pacific. (The first mode, which is substantially different from the second mode, mainly captures the ENSO–type SST–U200 relation and is not discussed here.) Associated with the cooling in the tropics–subtropics and warming in

the extratropics are the weakening of the EAJ and the changes in the North Pacific U200 that are similar to the pattern shown in Fig. 1b. Thus, a stronger EAJ is accompanied by colder SST underneath. It should also be pointed out that the SVD pattern experiences very small change when the entire Northern Hemisphere SST is applied in the calculation. This suggests a weak tie of the EJA with the SSTs of the North Atlantic and northern Indian Ocean.

Figure 4 has shown an important feature: the EAJ has a weak association with Niño–3 SST but links closely to the NPSST. This feature also implies that the EAJ and ENSO link differently to the NPSST. Figure 4c indicates that the variation of the EAJ–NPSST association varies on time scales longer than those of ENSO. The interdecadal variability of this association and its role in the variations of APA climate require further investigations.

Shown in Fig. 5 is the patterns of time–lag correlation between the EAJ and grid–point SST. It can be seen from Fig. 5a that the EAJ is positively correlated to the previous September–November (SON–) SST in the subtropics south of EAJ. However, it tends to be negatively correlated with the extratropical SST to the north of EAJ. The dominant feature of Figs. 5b–c is that the EAJ is negatively and significantly correlated with the SST underneath but positively correlated with the western Pacific SST south of 15°N.

Figure 5a suggests an important relationship between the EAJ and the north–south SST gradient in the subtropics during the antecedent season. A warming in the subtropical western Pacific during the previous season is followed by a strong EAJ in DJF. This strong EAJ, in turn, intensifies the surface westerly (25–42°N) as seen from the simultaneous correlation between the EAJ and the zonal wind of 1000 mb (figures not shown). The intensifying surface wind causes strong mixing, evaporation, and probably upwelling in some regions, and decreases the SST as shown in Fig. 5b. The positive correlation band extending from tropical western Pacific to subtropical eastern Pacific is consistently associated with a weakening of the northeasterly trade winds over the ocean domains. For most of the Pacific, there is a strong relationship between SST and the intensity of surface winds. Since there is no apparent relationship between the EAJ and the following springtime U200 of the same region, the similarity in Figs. 5b–c is likely accounted for by

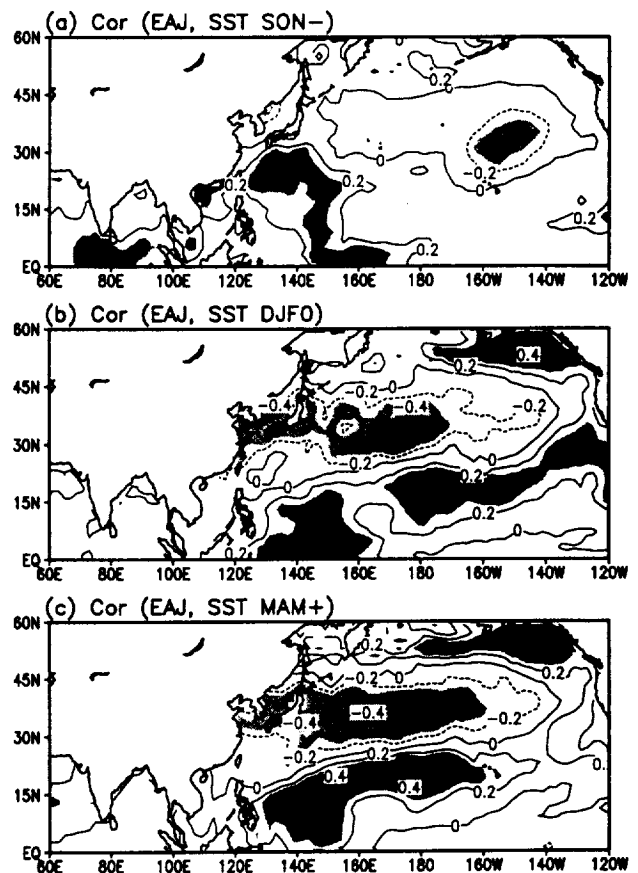the persistence of SST anomalies that have been formed during wintertime.

Fig. 5. Correlation between the EAJ and grid–point SST. Shown are the simultaneous pattern (b) and the patterns in which the SST leads the EAJ by one season (a) and lags the EAJ by one season (c). Values ≥ 95% confidence level are shaded.

4. Summary

In this study, we have demonstrated the importance of the wintertime EAJ for the variations of the APA climate. With an emphasis on the EAJ's association with the East Asian winter monsoon, tropical convection, upper tropospheric wave patterns, and the teleconnection patterns outside the extratropical Asian–Pacific region, we have discussed the relative contributions of the EAJ and ENSO to the climate anomalies of the APA region.

The EAJ and ENSO link to two very different modes of atmospheric circulation over the APA region. While ENSO causes robust, PNA–like signals to the east of the dateline, the EAJ links to a teleconnection pattern whose major climate anomalies appear over the Asian continent and

western Pacific (west of the dateline). A strong EAJ is accompanied clearly by a strong Asian winter monsoon that leads to cold climate over Asia and the Pacific and intensifying convection over the tropics. Changes in the EAJ are associated with broad–scale modification in the upper tropospheric wave patterns that lead to downstream climate anomalies over the eastern Pacific. Through this downstream influence, the EAJ causes climate signals in North America. Associated with a strong EAJ are the warming and less snow cover in the western but reverse anomalies in the eastern United States, although these signals are relatively weaker than the EAJ–related anomalies in East Asia.

The EAJ is closely associated with the NPSST that has little link to ENSO. An antecedent north–south SST gradient with warming in the tropics–subtropics and cooling in the extratropics of the western Pacific favors a strong EAJ. The accelerated EAJ is accompanied by intensifying low–level westerlies that lead to a decrease in the subtropical–extratropical SST. Such a SST anomaly lasts persistently from winter to the following spring, during which the local $U200$ has little link to the winter EAJ.

5. References

Bjerknes, J., A possible response of the atmospheric Hadley circulation to equatorial anomalies of ocean temperature. *Tellus,* **18**, 820–829.

Ceser, C., and M. L. Blackmon, 1995: On the relationship between tropical and North Pacific sea surface temperature variations. *J. Climate,* **8**, 1677–1680.

Chang, C.–P., and K.–M. Lau, 1980: Northeasterly cold surges and near–equatorial disturbances over winter MONEX area during December 1974: Part II: Planetary scale aspects. *Mon. Wea. Rev.,* **108**, 298–312.0.

Ding, Y.–H., 1992: Summer monsoon rainfalls in China. *J. Meteor. Soc. Japan,* **70**, 373–396.

Dong, M., J. Yu, and S. Gao, 1999: A study on the variations of the westerly jet over East Asia and its relation with the tropical convective heating. *Chinese J. Atmos. Sci.,* **23**(1), 62–70.

Huang, R., and K. Gambo, 1982: The response of a hemispheric multilevel model atmosphere to forcing by topography and stationary heat sources. *J. Meteor. Soc. Japan,* **60**, 78–108.

Kang, I.–S., and I.–M. Held, 1986: Linear and nonlinear diagnostic models of stationary eddies in the upper troposphere during northern summer. *J. Atmos. Sci.,* **43**, 3045–3057.

Kawamura, R., 1994: A rotated EOF analysis of global sea surface temperature variability with interannual and interdecadal scales. *J. Phys. Oceanogr.,* **24**, 707–715.

Lau, K.–M., G.–J. Yang, and S.–H. Shen, 1988: Seasonal and intraseasonal climatology of summer monsoon rainfall over East Asia. *Mon. Wea. Rev.,* **116**, 18–37.

Palmén, E., and C. W. Newton, 1969: Atmospheric Circulation Systems: Their Structure and Physical Interpretation. Academic Press, Inc., San Diego, California, pp. 603.

Plumb, R. A., 1985: On the three–dimensional propagation of stationary waves. *J. Atmos. Sci.,* **42**, 217–229.

Tao, S.–Y., and L.–X. Chen, 1987: A review of recent research of the east Asian summer monsoon in China. In *Monsoon Meteorology,* Ed. By C.–P. Chang and T. N. Krishnamurti, Oxford Univ. Press, pp. 60–92.

Webster, P. J., and S. Yang, 1992: Monsoon and ENSO: Selectively interactive systems. *Quart. J. Roy. Meteor. Soc.,* **118**, 877–926.

Yang, S., and W. J. Gutowski, 1994: GCM simulations of the three–dimensional propagation of stationary waves. *J. Climate,* **7**, 414–433.

Yang, S., and P. J. Webster, 1990: The effect of summer tropical heating on the location and intensity of the extratropical westerly jet streams. *J. Geophys. Res.,* **95**, 18705–18721.

Yeh, T.–C., S.–Y. Dao, and M.–T. Li, 1959: The abrupt change of circulation over the Northern Hemisphere during June and October. In *The Atmosphere and the Sea in Motion,* Ed. By B. Bolin, Rockefeller Inst. Press, New York, pp. 249–267.

Zeng, Q. C., 1979: Mathematical and Physical Basis for Numerical Weather Forecast. Science Press, Beijing, China, pp. 314.

*   SAIC/General Science Corporation, Beltsville, MD 20705, USA
** Universities Space Research Association, Seabrook, MD 20706, USA